Chemosphere 161 (2016) 510–517

Contents lists available at ScienceDirect

Chemosphere

journal homepage: www.elsevier.com/locate/chemosphere

Formation of microscopic particles during the degradation of different polymers

Scott Lambert*, Martin Wagner

Department Aquatic Ecotoxicology, Goethe University, Max-von-Laue-Str. 13, 60438, Frankfurt am Main, Germany

HIGHLIGHTS

- Degradation of seven polymers in aquatic medium results in an increased formation of microscopic plastic particles.
- Weathering of polystyrene and polylactic acid generated the highest number of particles, especially in the nanometer range.
- Surface erosion of all seven materials produced particles from 30 nm up to 60 μm.
- Particle concentration increased with decreasing particle diameter.
- Degradation processes start with chain scission at the polymer surface releasing many very small particles.

ARTICLE INFO

Article history:
Received 7 May 2016
Received in revised form
8 July 2016
Accepted 14 July 2016
Available online 25 July 2016

Handling Editor: Tamara S. Galloway

Keywords:
Nanoplastics
Microplastics
Degradation
Environment
Nanoparticle tracking analysis
Coulter counter

ABSTRACT

This study investigated the formation and size distribution of microscopic plastic particles during the degradation of different plastic materials. Particle number concentrations in the size range 30 nm–60 μm were measured by nanoparticle tracking analysis (NTA) and Coulter Counter techniques. Each of the plastics used exhibited a measureable increase in the release of particles into the surrounding solution, with polystyrene (PS) and polylactic acid (PLA) generating the highest particle concentrations. After 112 d, particle concentrations ranged from 2147 particles ml^{-1} in the control (C) to 92,465 particles ml^{-1} for PS in the 2–60 μm size class; 1.2×10^5 particles ml^{-1} (C) to 11.6×10^6 for PLA in the 0.6–18 μm size class; and 0.2×10^8 particles ml^{-1} (C) to 6.4×10^8 particles ml^{-1} for PS in the 30–2000 nm size class (84 d). A classification of samples based on principal component analysis showed a separation between the different plastic types, with PLA clustering individually in each of the three size classes. In addition, particle size distribution models were used to examine more closely the size distribution data generated by NTA. Overall, the results indicate that at the beginning of plastic weathering processes chain scission at the polymer surface causes many very small particles to be released into the surrounding solution and those concentrations may vary between plastic types.

1. Introduction

It has recently been shown that indicators of anthropogenic activity in lake sediments include a complex combination of materials, including plastics, and that these indicators differ greatly from Holocene signatures (Waters et al., 2016). As such, the environmental degradation of different plastic materials is of great interest. Conventional understanding regarding plastic degradation processes is derived from laboratory studies that often investigate a single mechanism of degradation such as photo-, thermal-, or biodegradation (Lambert et al., 2013b). These studies have tended to focus on thin films and characterise degradation in terms of weight loss, changes in tensile strength, breakdown of molecular structure, and the identification of specific microbial strains to utilize specific polymer types. Presently, little is known about the formation of microscopic particles during the degradation of different plastic materials. This is an important issue given the current interest in the environmental occurrence and effects of microplastics that are generally classified as having a diameter less than 5 mm (GESAMP, 2015). In addition, the formation of particles below the threshold of visible detection, such as those at the nanoscale, during plastic degradation is also considered highly likely (Andrady, 2011; Lambert et al., 2014; Mattsson et al., 2015).

* Corresponding author.
E-mail addresses: scottl210@hotmail.co.uk, lambert@em.uni-frankfurt.de (S. Lambert).

http://dx.doi.org/10.1016/j.chemosphere.2016.07.042
0045-6535/

Analytical methods for particle characterisation include Coulter Counter and nanoparticle tracking analysis (NTA). Coulter Counter is a conductivity based technique that is able to measure particles ranging from 0.4 to 1200 μm diameter depending on the size of aperture used (Rhyner, 2011). The sample of interest is diluted in a weak electrolyte solution and is then passed through the aperture concurrent with an electrical current. The voltage applied across the aperture is known as the sensing area and as particles pass through the aperture they displace their own volume of electrolyte and alter the impedance (Demeule et al., 2010; Narhi et al., 2009). This change in impedance produces a pulse that is directly proportional to the volume of the particle and this converted signal enables the instrument to calculate particle size and size distribution (Demeule et al., 2010; Narhi et al., 2009).

NTA visualizes, measures, and characterises particles in the 30–2000 nm size range through the use of a laser beam to illuminate particles (Filipe et al., 2010). The NTA technique is based on the tracking of single particles and the software relates the rate of Brownian motion to particle size. The scattered light is captured using a digital camera and the motion of each particle is tracked from frame to frame by the NTA software (Kramberger et al., 2012). The rate of particle movement is related to a sphere equivalent hydrodynamic radius as calculated through the Stokes-Einstein equation and particle size is observed on a particle-by-particle basis (La Rocca et al., 2014). The principles of NTA are further described in Hole et al. (2013), Gillespie et al. (2011), and Gallego-Urrea et al. (2010). The NTA platform has previously been used to investigate the particle formation during the degradation of natural rubber latex (Lambert et al., 2013a) and polystyrene (Lambert and Wagner, 2016).

The size distribution of particles in aquatic environments is an important property that influences many natural processes, such as the scattering and absorption of light in the water column, the exchange of substances between solid and liquid phases, and the transportation of substances to sediments, as well as their interactions with biological processes (Jonasz, 1983; Reynolds et al., 2010). A particle size distribution (PSD) can be defined as the average number of particles within a given size classification (Reynolds et al., 2010). In addition, modelling the size distribution of particles is often useful when highly variable particle populations are expected as they can provide a more complete description of PSD properties (Hwang et al., 2002). Therefore, an investigation of PSD of plastic particles formed during degradation processes is of particular interest, and representing the particle concentration data as a mathematical function may provide an opportunity to search for materials with similar degradation profiles.

In this study, we aimed to investigate the formation of microscopic particles during the degradation of different plastic materials, under aqueous conditions. To do this, a weathering chamber was used to accelerate the degradation process, and seven plastic materials were compared that represented five different polymer types. The materials selected consisted of two plastic pellets (polyethylene (PE) and polypropylene (PP)), and five consumer plastics including two types of PP packaging materials, a polystyrene (PS) coffee-to-go lid, a polyethylene terephthalate (PET) water bottle, and a polylactic acid (PLA) beverage cup. The main objective was to characterise the formation of particles from 30 nm to 60 μm in diameter and to explore the effects of polymer type on particle formation. A second objective was to further examine the particle distribution data generated by NTA within the context of commonly used PSD modelling approaches.

2. Methods

2.1. Test materials and their preparation

The plastic pellets used in this work were purchased from a commercial source and the consumer plastics were sourced from commercial retailors in Darmstadt, Germany (supporting information (SI) Table S1). The polymer type of the consumer plastics were identified through their recycling code, and the identification of all materials was further confirmed using ATR-FTIR spectroscopy (Attenuated Total Reflection-Fourier Transform Infra-Red, PerkinElmer UATR Two; the individual spectra are available in the SI Fig. S1). The plastics used were durable materials and not those associated with thin film materials.

The consumer plastics were emptied and plastic material covered by labelling was cut away and not used to exclude any glue residues. The remaining plastic material was then gently washed under a running demineralised water tap, with care taken to prevent artificial disturbance of the material surfaces. After drying the consumer plastics were then cut into 1 × 1 cm squares using stainless steel scissors. The plastic materials were then placed in glass vials, immersed in 20 ml demineralised water, and placed in a weathering chamber (Binder GmbH). The exposure conditions were kept static with the temperature set to 30 °C and continuous exposure to light in both the visible and ultra-violet (UV; 320–400 nm) range. Samples were taken after 0, 7, 14, 28, 56, 84, and 112 days, for each time point individual samples were established in triplicate alongside control samples (i.e. water only). Evaporation was dealt with by regularly replacing lost water. For the consumer plastics each individual replicate contained one, 1 × 1 cm square of material, and for the plastic pellets each individual replicate contained five pellets. The average surface area was as follows; 1.96 cm^2 for the five pellets (0.4 cm^2 per pellet), 2.03 cm^2 for the PP film, 2.12 cm^2 for the PP sheet, and 2.06 cm^2 for the three remaining materials. A laboratory blank of 20 ml demineralised water was prepared in a fresh glass vessel on the day of each sample collection to document any contamination that may result from the analytical process.

2.2. Analytical methods

To characterise the formation of plastic particles during the degradation of different plastic materials two methods were utilised: (i) Coulter Counter was used to determine the particle concentrations in the 0.6–60 μm size range, and (ii) NTA was used to determine particle size concentrations in the size range of 30–2000 nm. Coulter Counter measurements were performed using a Multisizer 3 equipped with a 30 μm and 100 μm aperture (Beckman Coulter, Fullerton, CA, USA). The 100 μm aperture allows particles with a diameter of 2–60 μm to be counted, and the 30 μm aperture allows for the counting of 0.6–18 μm particles. Liquid samples were diluted between 20 and 50 fold with Isoton II electrolyte (ISO; 0.9% NaCl electrolyte from Beckman Coulter) solution to provide adequate ionic strength for the analysis. To adequately characterise particle concentration each individual sample, control, and blank were analysed in triplicate with each aperture.

NTA analysis was performed using NanoSight LM 10 (NanoSight Ltd, Wiltshire, UK). Only samples generated from days 0–84 were analysed by NTA because of unexpected instrument down time. To characterise each individual replicate sample, control, and blank in a representative manner three video images of each were taken and designated as a single measurement. Video image length was set at 30 s and imaging was performed at room temperature. The video images were then processed using NTA 2.3 software with the following parameters; detention threshold set to auto; blur set to

5 × 5; minimum track length and minimum expected particle size were both set to auto. During the particle tracking analysis two output files for each image are generated. The first is the summary output file that contains data such as the particle concentration and the *x*, *y* data points from which the particle concentration distribution can be recreated. The second file is the intensity output file and that contains data on the particle diameter of each individual particle tracked during the analysis, and whether the particle is considered a true particle and included in the data that makes up the summary file or a false particle and excluded.

2.3. Data analysis

The datasets generated for the three size classes investigated were identified as non-normally distributed using the Shapiro-Wilk test. Therefore, overall differences in particle concentrations between the treatment groups and control were evaluated using Kruskal-Wallis on ranks. Statistical tests were followed by *post-hoc* Dunn's test for multiple comparisons, and were conducted using GraphPad Prism version 5.0 and a significance level of 0.05. The particle concentration data were then normalized to surface area and further characterized using principal component analysis (PCA), which reduces the complexity of a multivariable dataset, and Spearman rank correlation. The goal of this approach was to provide an overview of the generated particle concentration data to identify similarities or differences between the treatment groups. PCA was performed using XLSTAT (Addinsoft, Inc, NY, USA), and the correlation analysis was performed using GraphPad Prism (version 5.0).

To further interpret the NTA data PSD modelling approaches were adopted. The NTA intensity files were exported to Microsoft Excel, where the pivot table function was used to exclude all measurements classified as false particles, so that only those particles classified as true particles were retained for PSD modelling. As three separate measurements of each replicate sample were analysed, particles classified as true from each were combined to create the particle distribution for that replicate sample. Generally, PSDs are reported as cumulative distributions frequencies (CDF) with different models proposed to fit the experimental data (Hwang. 2002). Therefore, a CDF of the particle size data obtained from the NTA intensity files was created in GraphPad Prism using a bin width of 10 nm. To characterise the CDF profiles four models were selected for regression analysis: Weibull distribution, exponential distribution, gamma distribution, and the van Genuchten power law distribution. These models each have two fitting parameters and are commonly used models for characterising particles distributions. Each of these models and their applications are further described in Bayat et al. (2015), Weipeng et al. (2015), and Yang et al. (2012). Model parameters were fitted using Microsoft Excel solver configured adopting recommendations of Brown et al. (2001) and recently employed by Prata et al. (2016). In addition, interpolation functions were also fitted to the measured data in the form of a second and third order polynomial models (Roberson and Weltje, 2014). To assess the models goodness-of-fit, R^2 value, root mean squared error (RMSE), and Akaike's information criterion (AIC) were used. In general, a given model is deemed to have a better goodness-of-fit when compared to other models if it has a higher R^2, and a lower RMSE and AIC. Equations are available in the supporting information.

3. Results

3.1. Analysis of laboratory blank samples

A laboratory blank consisting of demineralised water was created on the day of each sample collection to document any contamination that may result from sample handling and analytical processes (SI Fig. S2). In the largest size class (2–60 μm) mean particle concentrations ranged from a low of 425 particles ml^{-1} on day zero to a high of 10,164 particles ml^{-1} on day 14. In the 0.6–18 μm size class mean particle concentrations ranged from 5907 particles ml^{-1} on day 28–43,107 particles ml^{-1} on day 7, and in the smallest size class (30–2000 nm) particle concentrations ranged from 0 particles ml^{-1} on day 0 and day 84–86,670 particles ml^{-1} on day 7.

3.2. Effects of plastic type on particle formation

The Coulter Counter technique was used to characterise the formation of particles in two size classes (i.e. 2–60 μm and 0.6–18 μm). In the largest size class, based on the particle concentration data measured on day 112 the different plastic types can be ranked in order from highest to lowest particle generation as follows: PS (92,465 particles ml^{-1}) > PLA (61,750) > PP sheet (46,270) > PE pellet (39,619) > PP pellet (26,380) > PET (25,046) > PP film (24,323) > control (2,147). The plastic material with the largest surface area (PP sheet) is placed third in the ranking, while the PP film with the smallest surface area is shown to produce the lowest number of particles of the plastic materials investigated at the end of the study. The PE and PP pellets are ranked fourth and fifth, respectively. It is only for PLA (Fig. 1) that a maximum concentration is measured at the end of the study, though this is still lower than concentrations observed for PS (SI Fig. S3). Maximum concentrations were determined in the PE pellet sample at day 56 (152,668 particles ml^{-1}) and in the PP film sample at day 28 (78,564 particles ml^{-1}; Fig. S3), after which particle concentrations steadily declined. Prominent peaks can be seen for PS at day 28 (132,058 particles ml^{-1}) and for the PP sheet at day 84 (38,672 particles ml^{-1}; SI Fig. 3). The particle number distributions show that the majority of particles measured in the 2–60 μm size class occur at the lower end of the distribution (Fig. 1; day 90 values for PLA and PET are 4.8 and 4.3 μm, respectively, further details in the SI). The particle abundance increases exponentially with decreasing particle size and the PVD can be used to represent the presence of larger particles in the sample.

To further investigate the particle distributions a smaller aperture was used. The increase in particle concentrations over the study duration is clearer to visualize in the 0.6–18 μm size class (Fig. 2; day 90 values for PLA and the PP film are 1.16 and 1.18 μm, respectively, further details in the SI), with the exception of the PP film material, the particle concentrations are all greatest on day 112 (Fig. S4). At the end of the study the different plastic materials can be ranked highest to lowest based on the particle concentration data as follows: PLA (11.6×10^6 particles ml^{-1}) > PP pellet (10.3×10^6) > PS (9.9×10^6) > PP film (9.8×10^6) > PET (9.4×10^6) > PP sheet (8.9×10^6) > PE pellet (8.0×10^6) > control (1.2×10^5). In this size class, the PP sheet is placed sixth in the ranking and the PP film is ranked fourth, while the PP pellet is ranked above the PE pellet and PS is ranked third and PLA first.

The characterisation of the particle concentration datasets can be further explored by visualization in principal component space and correlation analysis after normalization based on surface area. The resulting two-component model (Fig. 3) of the different treatment groups reveal a division between the different plastic treatment groups, while the pair-wise correlation analyses (SI Table S2) describes the correlation between the plastic types in terms of their correlation coefficients. The similarities and differences between the different plastic treatments are clearest in the 2–60 μm size class. Here, four groups can be identified: group one consists of the PP sheet and PET with negative PC 1 scores and

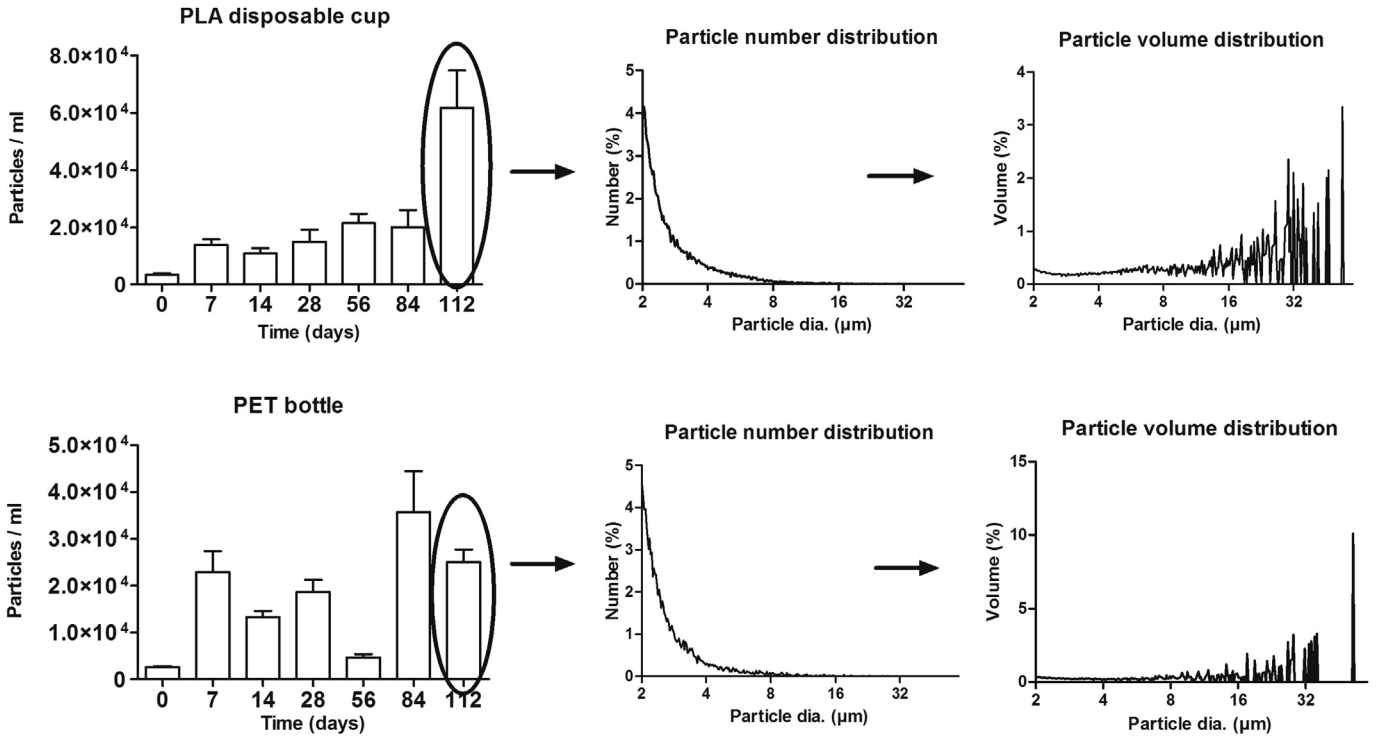

Fig. 1. Particle concentrations measured in the PLA and PET samples in the 2–60 µm size range, with accompanying number and volume distributions for day 112. Details for all other plastic materials and control data are presented in the supporting information.

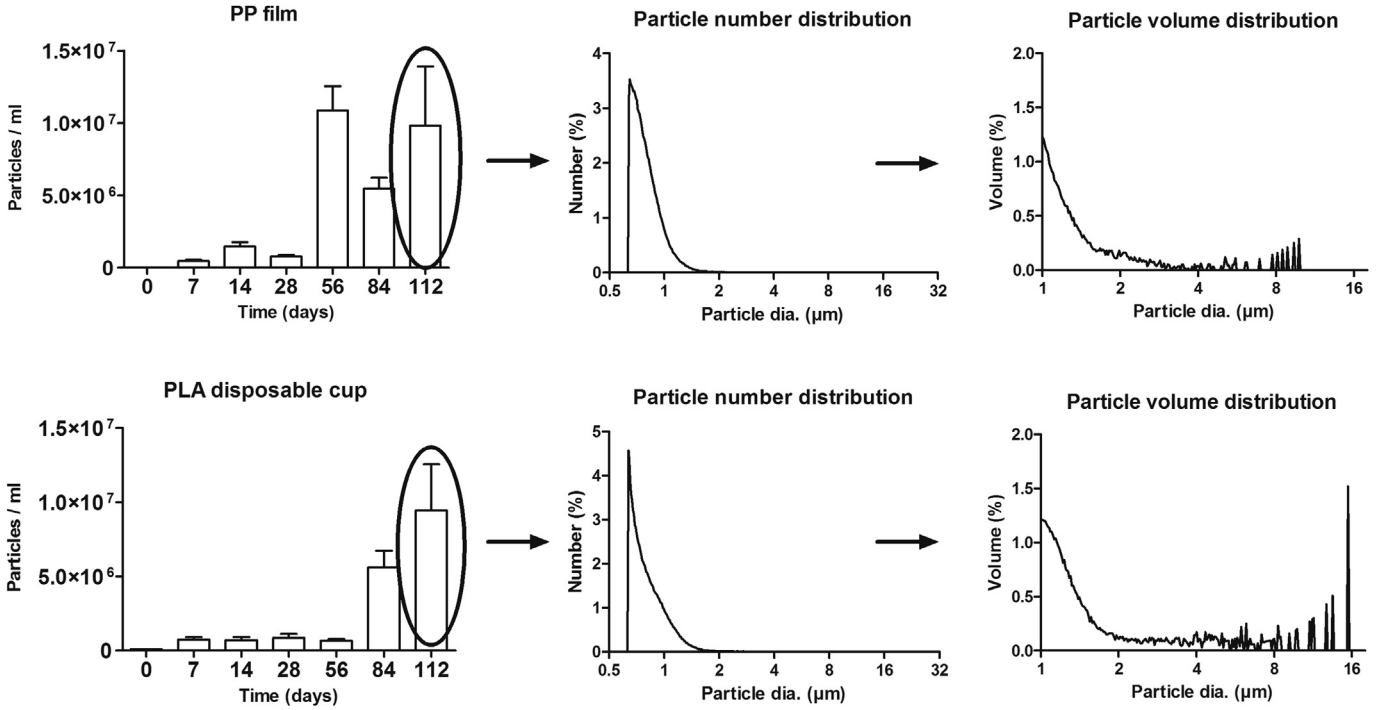

Fig. 2. Particle concentrations measured in the PLA and PP film samples in the 0.6–18 µm size range, with accompanying number and volume distributions for day 112. Details for all other plastic materials and control data are presented in the supporting information.

highly positive PC 2 scores (correlation coefficient of 0.69), group two consists of PS, the PE pellet and the PP film with positive PC 1 and PC 2 scores (correlation coefficient of 0.465–0.679), while PLA (negative PC 1 and PC 2 scores) and the PP pellet (positive PC 1 and negative PC 2 scores) form their own groups. The 2–60 µm size class is also the most complex dataset, because of the lower variance accounted for by the first two components (57.4%; Fig. 3) as compared to the 0.6–18 µm (78.2%) and the 30–2000 nm (79.4%)

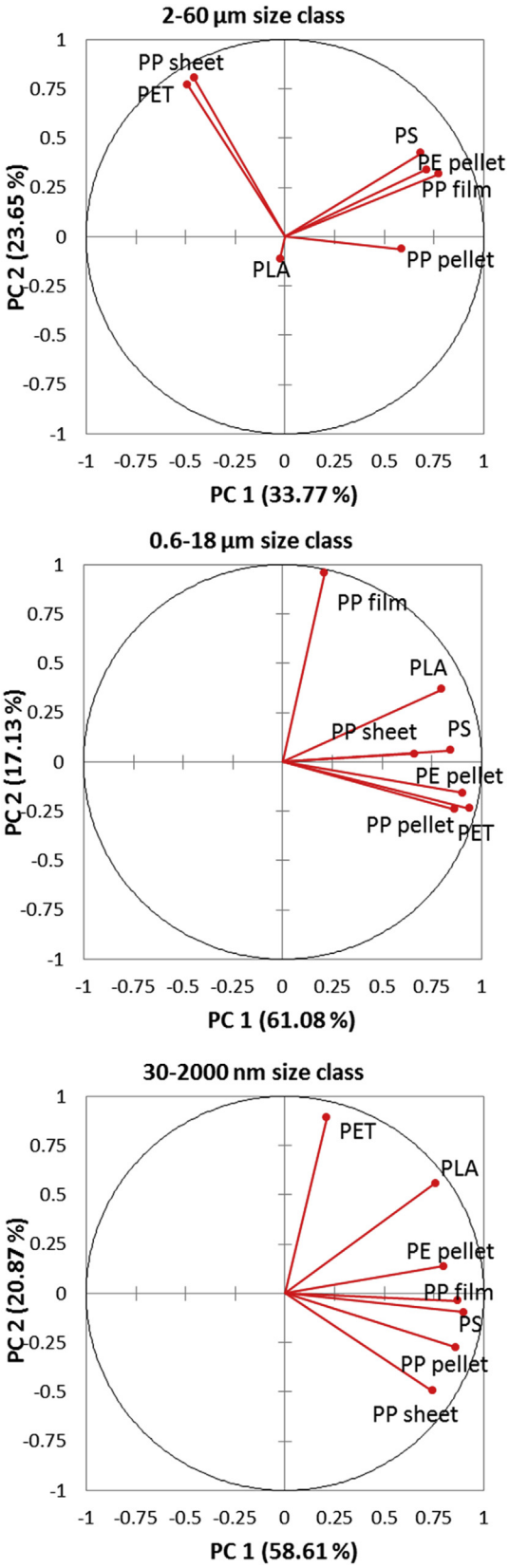

Fig. 3. Projection of the particle concentrations after normalization for surface area in principal component space for the different size classes investigated.

datasets. In the 0.6–18 µm size class the four groups can again be identified. The PE and PP pellets with PET cluster together with highly positive PC 1 and negative PC 2 scores (correlation coefficient of 0.744–0.752), the PP sheet and PS cluster together with highly positive PC 1 and positive PC 2 scores (correlation coefficient of 0.83), while the PP film and PLA form their own individual groups.

3.3. Characterisation of particle distributions at the nanoscale

NTA was used to investigate the formation of particles in the 30–2000 nm size range. Fig. 4 shows the particle volume distributions (PVD) generated in the PLA, PET, PS and control samples. The PVDs for all other plastics are presented as part of the supporting information. The concentration of particles measured in the solutions increased over the study duration and became increasingly influenced by particles at the lower end of the size distribution. This is best shown in the PS and PE pellet samples where the PVD is more influenced by larger particles at day 28, but after 84 days of weathering the PVD becomes more heavily influenced by particles at the lower end. This is possibly due to a number of factors such as the fragmentation of larger particles, and the ongoing weathering processes favoring the formation of smaller particles. When comparing plastics of similar densities an interesting comparison can be made between PET (1.34–1.39 g cm^{-3}) and PLA (1.21–1.43 g cm^{-3}). In the PLA samples the PVDs for days 7 and 28 are very similar and the concentration of particles is relatively low, whereas for the PET samples there is a notable difference in the PVD over this time period. However, after 84 days the PVD in the PLA samples markedly increases whereas in the PET it remained relatively stable.

At the end of the study the different plastic materials can be ranked in order from highest to lowest particle generation as follows: PS (6.4×10^8 particles ml^{-1}) > PLA (5.3×10^8) > PE pellet (3.4×10^8) > PP film (1.8×10^8) > PET (1.7×10^8) > PP pellet (1.7×10^8) > PP sheet (1.5×10^8) > control (0.2×10^8). In this size class the PP sheet with the largest surface area is ranked lowest out of the plastic materials, while PS and PLA are ranked first and second respectively. Overall, the results show a clear difference in particle concentrations between the control samples as compared to the plastic treatment groups. The clustering of different plastic treatments is not so obvious in this size class (Fig. 3). PET and PLA clearly cluster individually, while there is a steady separation between the remaining treatments starting with the PE pellet (highly positive PC 1 and positive PC 2 scores) through to the PP sheet (positive PC 1 and negative PC 2 scores). The results from the pairwise correlation analyses shows that the correlation between the plastics ranged from 0.2 (PET vs PP pellet) to 0.798 (PP sheet vs PP pellet).

The selected CDF models were fitted to the NTA data from the day 84 samples. The model that best described the measured CDF profiles for all seven plastics was the gamma distribution with R^2 values of 0.98–0.99 and RMSE vales of 0.023–0.029, whereas the third order polynomial had R^2 values of 0.93–0.97 and RMSE of 0.041–0.061. The least favourable models were the second order polynomial model (R^2 values of 0.77–0.90) and the Weibull distribution (R^2 values of 0.82–0.87; Table S3). The best-fitting model parameters are also provided in SI (Table S4). The CDF curves generated by the different models can also be discussed in terms of how well they predict PSD properties, such as mean particle diameter. Here, the gamma distribution was shown to provide the best prediction of the measured CDF mean particle diameter (Table S5). The CDF curves provided by the gamma and power law models are both fairly similar in their geometry for all plastic types; although the power law model tends to predict a lower mean particle size compared to the gamma model and measured data (Table S5). The exponential model over predicts the mean particle

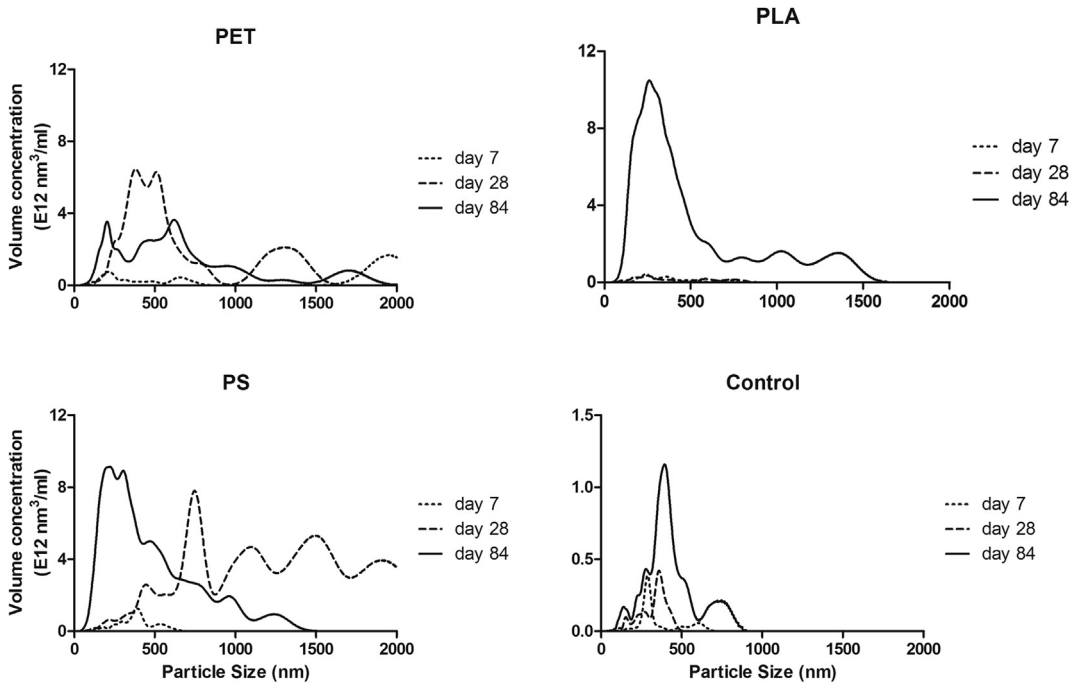

Fig. 4. Particle volume distributions measured by NTA for PET, PLA, PS, and the control samples. The particle volume distributions of the remaining plastics can be found in the supporting information.

size for all plastics except PET, and the geometry of the Weibull model means that it predicts the lowest mean particle size for all plastic types. Comparing the CDF curves of the two plastic pellets the PP pellet is shown to have a larger portion of particles below 100 nm contributing to its PSD compared to the PE pellet and therefore has an overall lower mean particle size (Fig. 5). For plastic with similar densities the CDF curves for PET and PLA show that a larger portion of particles below 100 nm contribute to the PET particle distribution than for PLA (Fig. S8). This means that PET has an overall lower mean particle size compared to PLA (Table S5). In addition, PLA produced higher particle concentrations in all three size classes compared to PET.

4. Discussion

The present study aimed to investigate the formation of microscopic particles during the degradation of different plastic materials under accelerated weathering conditions in the laboratory. All plastics generated increasing numbers of particles over time, with PS and PLA often generating higher particle concentrations than other polymers. In addition, the replicate measurements become increasingly variable as time progressed. However, as evidenced by PCA, PLA clusters individually particularly in the 2–60 μm size class (Fig. 3). The variability between replicate measurements may be due in part to the specific structural features of the individual replicate samples used, such as an uneven distribution of pore spaces at the polymer surface, which cause different patterns of degradation within plastic type. In this case, the light absorbed by particles in the water column may enhance their further disintegration and degradation, while decreasing the irradiance for degrading the parent samples. The extent to which suspended particles influence these processes depends strongly on their size distribution (Jonasz, 1983). The increasing presence and distributional differences of particles and other chemical degradation products was also noted as influencing the degradation processes of replicate rubber latex samples (Lambert et al., 2013b).

This study indicates that at the beginning of weathering processes many very small particles fragment from the polymer

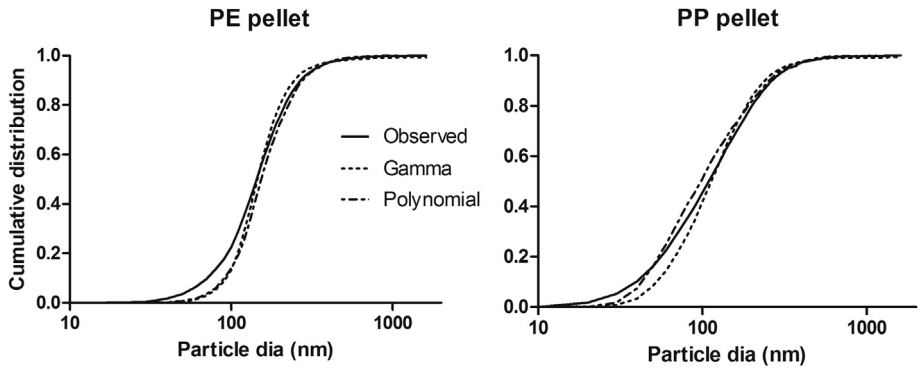

Fig. 5. Comparative fit of the gamma model and the 3rd order polynomial function used to describe the cumulative distribution for the PE and PP pellet particle concentrations measured after 84 days of artificial weathering.

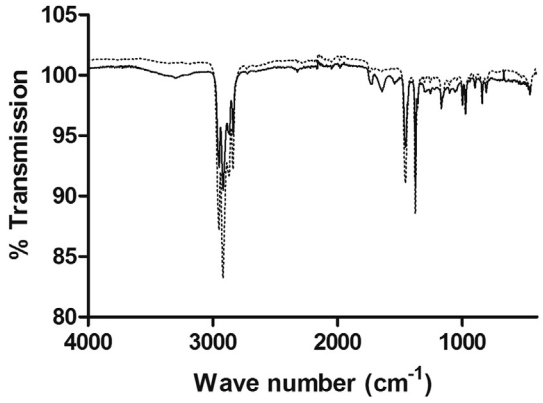

Fig. 6. FTIR spectra of the PP film sample at the start (dotted line) and end (day 112, solid line) of the study.

surface. The degradation pathways of PE, PLA, PP, PS, and PET were recently discussed in detail by Gewert et al. (2015) and Pelegrini et al. (2016). Generally, exposure to sunlight and oxygen are the most important factors that initiate polymer degradation, with chain scission at the polymer surface leading to the fragmentation of smaller polymer particles (Gewert et al., 2015; Lambert et al., 2014). This will in theory result in the core of the parent plastic becoming smaller and thinner. The complete fragmentation of the parent plastic will then occur at a much later point in time when it is sufficiently weakened. The FTIR spectra (Fig. 6 and Fig. S6 SI Fig. 1) show that all plastic materials display a weakening of their characteristic absorbance bands the formation of a broad OH peak in the region 3000–3600 cm^{-1}, and a low intensity peak at 1715 cm^{-1} that suggests the introduction of a CO band. SEM images are also available in Lambert and Wagner. (2016) that show a change in the surface of the PS material used.

Overall, the rate of particle formation will depend on the specific nature of the plastic material including the amount and size of pre-existing surface pore spaces, and surface stability. The number and size of surface pore spaces depends on the polymer crystallinity and in turn the polymer density (Rabek, 1975). Chain scission at the polymer surface during weathering processes will again depend on the degree of polymer crystallinity as well as the mobility and stiffness of chain segments (Rabek, 1975). Crystallinity is an important polymer property because the crystalline region consists of more ordered and tightly structured polymer chains. Crystallinity affects physical properties such as density and water permeability. This in turn affects their hydration and swelling behaviour. Previous studies have also shown that the chemical diversity of plastic materials leads to a complex mixture of degradation products that are difficult to quantify (Bejgarn et al., 2015; Lambert et al., 2013b).

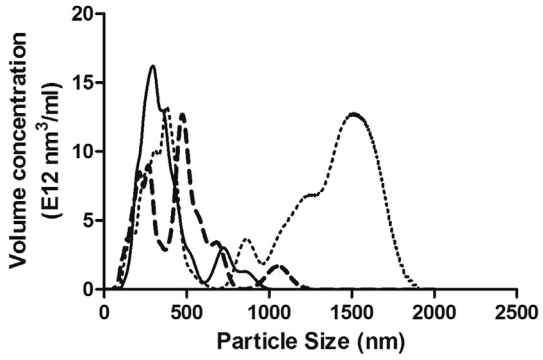

Fig. 7. Particle volume distribution of natural nanoparticles in a sample of freshwater (5.65×10^8 particles $ml^{-1} \pm 0.74$; n = 3). The sample was collected from a local river (Urselbach in Frankfurt, Germany) in September 2015.

The particle size distributions generated by all seven plastic types display an increase in particle concentration with decreasing particle diameter, and greater variability between the replicate measurements with increasing particle size. This trend may also be observed when monitoring PSDs in natural water samples (Peng et al., 2009; Reynolds et al., 2010). Gordon (1970) showed that particles are numerically more abundant at smaller sizes (<7 μm) during a study or organic particles in the North Atlantic Ocean using periodic acid schiff staining methods. However, Sheldon et al. (1972) presented data that showed roughly equal concentrations of particles occur within all size classes using Coulter Counter (1 μm was the smallest particle size and they studied surface and deep water samples from the Atlantic and Pacific Oceans). To put the particle concentrations into a broader context the PVD of natural nanoparticles in a freshwater sample was analysed (Fig. 7). The particle concentration measured was 5.65×10^8 particles ml^{-1}. The particle number concentrations of natural nanoparticles in aquatic environmental samples has been found to range from $0.5–20 \times 10^8$ particles ml^{-1} (Gallego-Urrea et al., 2010).

This study provides a base for further research on particle fragmentation during plastic weathering and degradation, for example particle formation may differ under different exposure conditions. During studies using natural rubber samples Lambert et al. (2013a) observed higher particle concentrations in freshwater as compared to marine water in outdoor microcosms. In addition, the exclusion of light and season (summer vs. winter) also affected the particle concentrations. The exposure conditions used in this study do not mimic actual environmental conditions, in which environmental plastics will be exposed to differences in light/dark cycles and temperature gradients. Rabek. (1975) reflected that polymer degradation is also influenced by the degree of thermal expansion. In this case, an interesting extension of this study would be to investigate temperature gradient and its effect on particle formation. Other important variables that will influence particle formation rates are polymer properties such as density and crystallinity, the type and quantity of chemical additives, and microbial communities.

Acknowledgments

This project has received funding from the European Union's Horizon 2020 research and innovation programme under the Marie Skłodowska-Curie grant agreement No 660306. We would also to thank Dr Robert Tampé at the Institute of Biochemistry, Goethe University Frankfurt for access to the NanoSight.

Appendix A. Supplementary data

Supplementary data related to this article can be found at http://dx.doi.org/10.1016/j.chemosphere.2016.07.042.

References

Andrady, A.L., 2011. Microplastics in the marine environment. Mar. Pollut. Bull. 62, 1596–1605.
Bayat, H., Rastgo, M., Mansouri Zadeh, M., Vereecken, H., 2015. Particle size distribution models, their characteristics and fitting capability. J. Hydrol. 529, 872–889. Part 3.
Bejgarn, S., Macleod, M., Bogdal, C., Breitholtz, M., 2015. Toxicity of leachate from weathering plastics: an exploratory screening study with Nitocra spinipes. Chemosphere 132, 114–119.
Brown, D.M., Wilson, M.R., Macnee, W., Stone, V., Donaldson, K., 2001. Size-dependent proinflammatory effects of ultrafine polystyrene particles: a role for

surface area and oxidative stress in the enhanced activity of ultrafines. Toxicol. Appl. Pharmacol. 175, 191–199.
Demeule, B., Messick, S., Shire, S.J., Liu, J., 2010. Characterization of particles in protein solutions: reaching the limits of current technologies. AAPS J. 12, 708–715.
Filipe, V., Hawe, A., Jiskoot, W., 2010. Critical evaluation of nanoparticle tracking analysis (NTA) by NanoSight for the measurement of nanoparticles and protein aggregates. Pharm. Res. 27, 796–810.
Gallego-Urrea, J.A., Tuoriniemi, J., Pallander, T., Hassellov, M., 2010. Measurements of nanoparticle number concentrations and size distributions in contrasting aquatic environments using nanoparticle tracking analysis. Environ. Chem. 7, 67–81.
GESAMP, 2015. Sources, Fate and Effects of Microplastics in the Marine Environment: a Global Assessment. Joint Group of Experts on the Scientific Aspects of Marine Environmental Protection [Online], Reports and studies 90. Available. http://ec.europa.eu/environment/marine/good-environmental-status/descriptor-10/pdf/GESAMP_microplastics%20full%20study.pdf.
Gewert, B., Plassmann, M.M., Macleod, M., 2015. Pathways for degradation of plastic polymers floating in the marine environment. Environ. Sci-Processes Impacts 17, 1513–1521.
Gillespie, C., Halling, P., Edwards, D., 2011. Monitoring of particle growth at a low concentration of a poorly water soluble drug using the NanoSight LM20. Colloids SurfacesPhysicochem. Eng. Aspects 384, 233–239.
Gordon, D.C., 1970. A microscopic study of organic particles in the North Atlantic ocean. Deep Sea Res. Oceanogr. 17, 175–185.
Hole, P., Sillence, K., Hannell, C., Maguire, C.M., Roesslein, M., Suarez, G., Capracotta, S., Magdolenova, Z., Horev-Azaria, L., Dybowska, A., Cooke, L., Haase, A., Contal, S., Mano, S., Vennemann, A., Sauvain, J.-J., Staunton, K.C., Anguissola, S., Luch, A., Dusinska, M., Korenstein, R., Gutleb, A.C., Wiemann, M., Prina-Mello, A., Riediker, M., Wick, P., 2013. Interlaboratory comparison of size measurements on nanoparticles using nanoparticle tracking analysis (NTA). J. Nanoparticle Res. 15.
Hwang, S.I., Lee, K.P., Lee, D.S., Powers, S.E., 2002. Models for estimating soil particle-size distributions. Soil Sci. Soc. Am. J. 66, 1143–1150.
Jonasz, M., 1983. Particle-size distributions in the baltic. Tellus B 35, 346–358.
Kramberger, P., Ciringer, M., Strancar, A., Peterka, M., 2012. Evaluation of nanoparticle tracking analysis for total virus particle determination. Virol. J. 9.
La Rocca, A., Di Liberto, G., Shayler, P.J., Parmenter, C.D.J., Fay, M.W., 2014. Application of nanoparticle tracking analysis platform for the measurement of soot-in-oil agglomerates from automotive engines. Tribol. Int. 70, 142–147.
Lambert, S., Sinclair, C.J., Boxall, A.B.A., 2014. Occurrence, degradation and effects of polymer-based materials in the environment. Rev. Environ. Contam. Toxicol. 227, 1–53.
Lambert, S., Sinclair, C.J., Bradley, E.L., Boxall, A.B.A., 2013a. Effects of environmental conditions on latex dergadation in aquatic systems. Sci. Total Environ. 447, 225–234.
Lambert, S., Sinclair, C.J., Bradley, E.L., Boxall, A.B.A., 2013b. Environmental fate of processed natural rubber latex. Environ. Sci. Process. Impacts 15, 1359–1368.
Lambert, S., Wagner, M., 2016. Characterisation of nanoplastics during the degradation of polystyrene. Chemosphere 145, 265–268.
Mattsson, K., Hansson, L.A., Cedervall, T., 2015. Nano-plastics in the aquatic environment. Environ. Sci. Process. Impacts 17, 1712–1721.
Narhi, L.O., Jiang, Y., Cao, S., Benedek, K., Shnek, D., 2009. A critical review of analytical methods for subvisible and visible particles. Curr. Pharm. Biotechnol. 10, 373–381.
Pelegrini, K., Donazzolo, I., Brambilla, V., Grisa, A.M.C., Piazza, D., Zattera, A.J., Brandalise, R.N., 2016. Degradation of PLA and PLA in composites with triacetin and buriti fiber after 600 days in a simulated marine environment. J. Appl. Polym. Sci. 133.
Peng, F., Effler, S.W., Donnell, D.O., Weidemann, A.D., Auer, M.T., 2009. Characterizations of minerogenic particles in support of modeling light scattering in Lake Superior through a two-component approach. Limnol. Oceanogr. 54, 1369–1381.
Prata, J.R.A.A., Santos, J.M., Beghi, S.P., Fernandes, I.F., Vom Marttens, L.L.C., Pereira Neto, L.I., Martins, R.S., Reis, J.R.N.C., Stuetz, R.M., 2016. Dynamic flux chamber measurements of hydrogen sulfide emission rate from a quiescent surface – a computational evaluation. Chemosphere 146, 426–434.
Rabek, J.B., 1975. Oxidative degradation of polymers. In: Bamford (Ed.), Comprehensive Chemical Kinetics Volume 14: Degradation of Polymers. Elsevier Scientific Publishing Company, Amsterdam, Netherlands.
Reynolds, R.A., Stramski, D., Wright, V.M., Woźniak, S.B., 2010. Measurements and characterization of particle size distributions in coastal waters. J. Geophys. Res. Oceans 115 (n/a-n/a).
Rhyner, M.N., 2011. The coulter principle for analysis of subvisible particles in protein formulations. AAPS J. 13, 54–58.
Roberson, S., Weltje, G.J., 2014. Inter-instrument comparison of particle-size analysers. Sedimentology 61, 1157–1174.
Sheldon, R.W., Prakash, A., Sutcliffe, W.H., 1972. The size distribution of particles in the ocean. Limnol. Oceanogr. 17 (3), 327–340.
Waters, C.N., Zalasiewicz, J., Summerhayes, C., Barnosky, A.D., Poirier, C., Galuszka, A., Cearreta, A., Edgeworth, M., Ellis, E.C., Ellis, M., Jeandel, C., Leinfelder, R., Mcneill, J.R., Richter, D., Steffen, W., Syvitski, J., Vidas, D., Wagreich, M., Williams, M., Zhisheng, A., Grinevald, J., Odada, E., Oreskes, N., Wolfe, A.P., 2016. The Anthropocene is functionally and stratigraphically distinct from the Holocene. Science 351.
Weipeng, W., Jianli, L., Bingzi, Z., Jiabao, Z., Xiaopeng, L., Yifan, Y., 2015. Critical evaluation of particle size distribution models using soil data obtained with a laser diffraction method. Plos One 10, e0125048.
Yang, X., Lee, J., Barker, D.E., Wang, X., Zhang, Y., 2012. Comparison of six particle size distribution models on the goodness-of-fit to particulate matter sampled from animal buildings. J. Air Waste Manag. Assoc. 62, 725–735.